Geosciences Journal
Vol. 15, No. 1, p. 71 − 81, March 2011
DOI 10.1007/s12303-011-0009-9

Crust and upper mantle structures of the region between Korea and Taiwan by surface wave dispersion study

Kwang-Hyun Cho* *Petroleum Technology Institute, Korea National Oil Corporation, Anyang 431-711, Republic of Korea*
How-Wei Chen *Institute of Geophysics, National Central University, Jhongli City, Taoyuan County, 32001, Taiwan*
Ik-Bum Kang *Korea Institute of Geosciences and Mineral Resources, Daejeon 305-350, Republic of Korea*
Sang-Hyun Lee *School of Earth and Environmental Sciences, Seoul National University, Seoul 151-747, Republic of Korea*

ABSTRACT: We have investigated the crust and upper-mantle shear velocity structures of the region between Korea and Taiwan by analyzing the path-averaged group-velocity dispersion characteristic curves derived from surface waves. The depth of the East China Sea between Korea and Taiwan is mostly less than 100 m. We selected data from earthquakes of magnitude greater than 6.0 that occurred in Taiwan from 1999 to 2007. We used data from 219 seismograms recorded at three-component broadband seismic stations in South Korea. We also used data from 19 events from South Taiwan for our study of crust and upper-mantle shear-wave velocity structures. By examining the wave period between 5 s and 100 s, the group velocities of Rayleigh waves and Love waves were inverted jointly. These waves were computed using the multiple filter technique (MFT) and using the single-station method. The inversion results from the dispersion curves provide a detailed one-dimensional velocity profile of the East China Sea. The main features of the derived velocity profile are: 1) the unconsolidated sediments surface layer shows a fairly low shear-wave velocity value; 2) the crustal shear-wave velocity increases from 2.92 km/s to 3.90 km/s, as the depth increases to 30 km; 3) shear-wave velocities in the uppermost mantle exhibit a clear low-velocity zone between 50 km and 90 km, with the velocity varying between 4.33 km/s and 3.99 km/s; 4) the variation in shear-wave velocities in the upper mantle increases with increasing depth. We can infer that the crustal structure of the study area is continental crust. The average Moho depth is 30 km beneath the East China Sea.

Key words: surface waves, group-velocity dispersion, Korea, Taiwan, multiple filter technique, crustal structure, upper-mantle structure

1. INTRODUCTION

This study presents a path-average shear velocity model obtained from the group velocity of surface waves on the Eurasian continental shelf between Taiwan and Korea. Previous studies in this area have used geophysical methods, such as magnetic, gravitational, sonobuoy seismic refraction, and ocean bottom seismometer (OBS) seismic refraction measurements (Ludwing et al., 1973; Leyden et al., 1973; Hirata et al., 1991; Li et al., 2001; Jiang et al., 2002; Lin et al., 2005; Fang and Liu, 2005; Han et al., 2007). However, previous seismic studies could not perfectly cover this study area without the distribution of event-station pairs crossing the East China Sea (Ludwing et al., 1973; Leyden et al., 1973; Hirata et al., 1991; Li et al., 2001). Because the event-station pairs are unique to Korean seismic stations, this study provides new information in this study area (Fig. 1).

Surface-wave group and phase-velocity investigations are being actively conducted the world over (Cho and Lee, 2006; Cho et al., 2007; Yoo et al., 2007; Nishida et al., 2008; Yang et al., 2010; Cho et al., 2011). The analysis technique provides important information on the properties of the crust and upper mantle in various regions of the Earth. Surface waves are most useful for studying structures in regions that are devoid of large-scale lateral property changes. The depth of the continental shelf in the East China Sea between Korea and Taiwan is mostly less than 100 m (Figs. 1 and 2). This makes the shelf appropriate for surface wave research. The long propagation distance between Korea and Taiwan makes it possible to compute group velocities of the surface wave by using the single station method, without needing to correct for errors due to the source mechanism (Panza et al., 1973, 1975a, 1975b). In addition, we have well-recorded seismic data from major events around South Korea and Taiwan that we can use for surface wave analysis.

We implemented the multiple filter technique (MFT) to obtain the group velocities of the surface wave fundamental-mode signal (Dziewonski et al., 1969; Herrmann, 1973). We determined the average shear-wave velocity structure between Korea and Taiwan by inverting the group velocity dispersion curve. Fundamental-mode Rayleigh wave and Love wave velocity data were inverted both separately and jointly. The goal of this paper is to study the properties of crust and upper-mantle structures of the East China Sea using surface wave analysis.

2. BROADBAND DATA COLLECTION FROM THE PAST SEVEN YEARS

For the purposes of examining the velocity model between

*Corresponding author: light123@knoc.co.kr

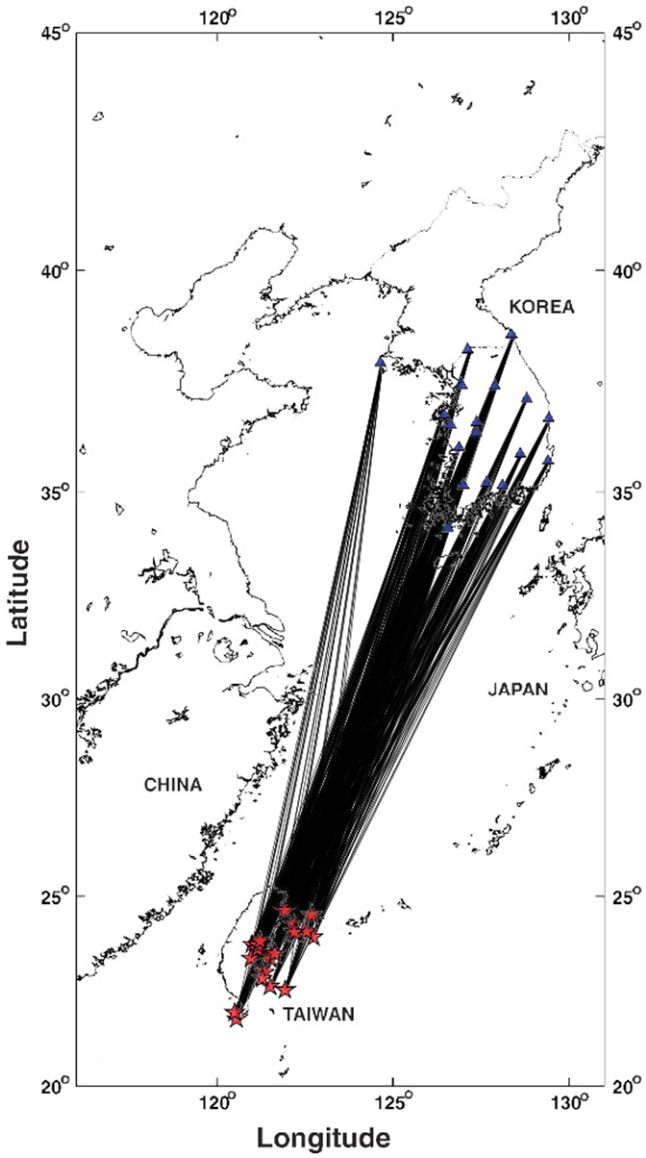

Fig. 1. The 19 earthquake events of Taiwan (red stars) and seismic stations (blue solid triangles) of South Korea. Ray paths (not show) connecting stations and earthquake events are mainly across the China-Korea-Japan borders.

South Korea and Taiwan, Figure 1 shows 19 events (details in Table 1) detected in Taiwan between September 1999 and January 2007. The data was recorded at broadband seismic stations in Korea. The seismic stations were part of the KIGAM-KERC (Korea Institute of Geosciences and Mineral Resources-Korea Earthquake Research Center) and KMA (Korea Meteorological Administration) stations. KIGAM and KMA operate stations equipped with STS-2 three-component broadband seismic sensors. From Figure 1, it is evident that the epicentral distance between seismic events and stations in Korea is approximately 1450 km to 2000 km, and that seismic waves mainly propagate across the East China Sea. Surface wave propagation across the East China Sea arises from a low-velocity waveguide for Love waves, and a stress-free surface for Rayleigh waves. In addition, the average ocean bottom bathymetry depth is approximately 100 m (Fig. 2). Therefore, we can ignore group delay due to the source mechanism and sea water depth, as the effects from the water layer ought to be relatively small.

Figure 3 shows a three-component seismogram recorded at station SNU. The well-recorded seismic event occurred at 21.80°N and 120.55°E on 26 December, 2006 (PingTung earthquake), based on the earthquake catalog of the USGS (United States Geological Survey). The quality of the original unfiltered data (Fig. 3a) is very high, which means that we only need to eliminate instrumental responses from records, using a deconvolution procedure. In addition, we can immediately identify clear Rayleigh wave and Love wave phases, obtained from radial and transverse components by vectorial rotation of two horizontal components, from their waveform amplitude and arrival times (Fig. 3b).

3. ANALYSIS

Figure 4 shows an interesting event. Here, we have a typical high signal-to-noise-ratio three-component seismogram for rare earthquake doublets recorded from an earthquake sequence in PingTung, southwest Taiwan. The equally spaced seismograms are arranged according to their corresponding epicentral distance. We obtained the radial and transverse components from a vector rotation of the two horizontal components. Though none of the three components of the recorded data are filtered, surface waves are dominant in every recorded seismogram. The distance between Korea and Taiwan has a sufficient boundary condition to make surface waves become prominent for dispersion and velocity structure studies. Rotated signals at each station show very distinctive seismic wave dispersion phenomena. In addition, predominantly large-amplitude surface waves, observed among individual permanent broadband stations traveling across the southern part of the Korean Peninsula, provide a valuable chance to study path-effect-related crust-to-mantle structures. After confirming that there was no lateral variation in the wave propagating paths, and then comparing the recorded data from Figures 3 and 4, we see that the Rayleigh wave identified from the radial component is very similar to the one from the vertical component. In addition, the Love wave identified from the transverse component has a faster phase and group velocity than the Rayleigh wave from the radial (vertical) component. In view of the clear phases, low noise contamination, apparent interstation traveling effect observed from recorded data, and no complications from the propagation effect, the group velocity analysis obtained from the rotated records using the multiple-filter method (Dziewonski et al., 1969; Herrmann, 1973) is straightforward.

Considering the high quality and quantity of the original

Table 1. List of hypocenter parameters for earthquakes occurring in Taiwan

Event	Date(dd/mm/yyyy)	Origin time(h:m:s)	Lat.(°N)	Long.(°E)	Depth(km)	Number of stations received	Magnitude
1	20/09/1999	17:47:18.5	23.77	120.98	33	4	7.70
2	22/09/1999	00:14:39.1	23.73	121.17	26	4	6.40
3	22/09/1999	00:49:42.8	23.64	121.14	33	4	6.20
4	25/09/1999	23:52:48.7	23.74	121.16	17	4	6.50
5	01/11/1999	17:53:00.1	23.38	121.52	33	4	6.30
6	10/06/2000	18:23:29.3	23.84	121.22	33	4	6.40
7	18/12/2001	04:02:58.3	23.95	122.73	14	6	7.30
8	31/03/2002	06:52:50.5	24.28	122.18	32	7	7.40
9	15/05/2002	03:46:05.8	24.64	121.92	10	8	6.20
10	28/05/2002	16:45:17.1	24.07	122.26	33	8	6.10
11	10/06/ 2003	08:40:30.8	23.52	121.63	44	7	6.00
12	10/12/2003	04:38:11.6	23.04	121.36	10	17	6.80
13	15/10/2004	04:08:50.2	24.53	122.69	94	18	6.70
14	08/11/2004	15:55:01.1	24.10	122.54	29	19	6.30
15	06/09/2005	01:16:02.3	24.08	122.19	32	19	6.10
16	01/04/2006	10 02 19.6	22.87	121.28	9	18	6.20
17	26/12/2006	12 26 21.1	21.80	120.55	10	20	7.30
18	26/12/2006	12 34 13.8	21.97	120.49	10	20	7.10
19	25/01/2007	10 59 17.6	22.56	121.93	36	18	6.00

The dataset were collected continuously over seven years soon after the Chi-Chi Taiwan earthquake caused severe damage in 1999. The number of broadband stations maintains a steady increase in S. Korea.

data records, we expect the group velocity dispersion curves of the Rayleigh waves derived from the vertical component to be consistent with those of the radial components (Figs. 3 and 4). For example, if we consider the data recorded at the SNU station, not only is the Raleigh wave group velocity (derived from both radial (red dots) and vertical components (blue dots)) consistent for the event occurring at 21.80°N and 120.55°E (Fig. 5a, Table 1), but it is also consistent for the event that occurred eight minutes later at 21.97°N and 120.49°E (Fig. 5b, Table 1) on 26 December, 2006. Consequently, we can obtain Love wave group velocity picks from the transverse component (green dots). Note that the first event has well-defined group velocities, up to a 100 s period, but this is not so for the second event. This is because interference limited the derived resolution, and therefore, we only used up to a 55 s period here. Clear Fourier amplitudes were usually large enough up to the 100 s period range to make all group-velocity measurements unambiguous. At a period ranging between 10 and 60 s, the similarity in the dispersion curves of the vertical and radial components of the Rayleigh waves means that the refraction of the surface wave does not occur in the paths. The dot symbols represent the chosen peaks from the group velocity stack after a two-dimensional grid search over the peak spectral amplitude in the phase velocity-period domain. The period range chosen for inversion, mainly between 5 and 100 s, is characteristic of the dispersion for earthquakes occurring in Taiwan. The distance between South Korea and Taiwan is relatively large, and the lower period is mainly controlled by the source excitation and the anelastic attenuation effect. As a result, we excluded short-period information (<5 s). The upper period limit is mainly affected by low-frequency noise content in the recorded signals.

For the PingTung earthquake doublets, we obtained group velocity data from Rayleigh and Love waves for all available data from the 20 broadband stations of the Korean Peninsula. Figure 6 shows the distribution of estimated group velocities at station SNU, including Rayleigh waves from the vertical (blue dots) and radial (gray dots) components, and Love waves (green dots) from the transverse component. For the same event, the distribution of group velocity variations for Rayleigh waves from both the vertical and radial components is almost identical, as the picked values overlap each other. Because the second event only occurs eight minutes later, fault reactivation or rupture complexity induced by the first event is highly possible. Even though rupture behaviors are somewhat different, when we compare their estimated group velocities from the first event (right) with those of the second (left) for a wave period between 5 and 55 s, we see that the distribution of the overall data values at the same (SNU) station are similar. Therefore this surface wave dispersion study using MFT associated with single station method provides a reliable solution from the well recorded individual datasets.

4. INVERSION AND RESULTS

The model we used as a basis for the surface-wave dis-

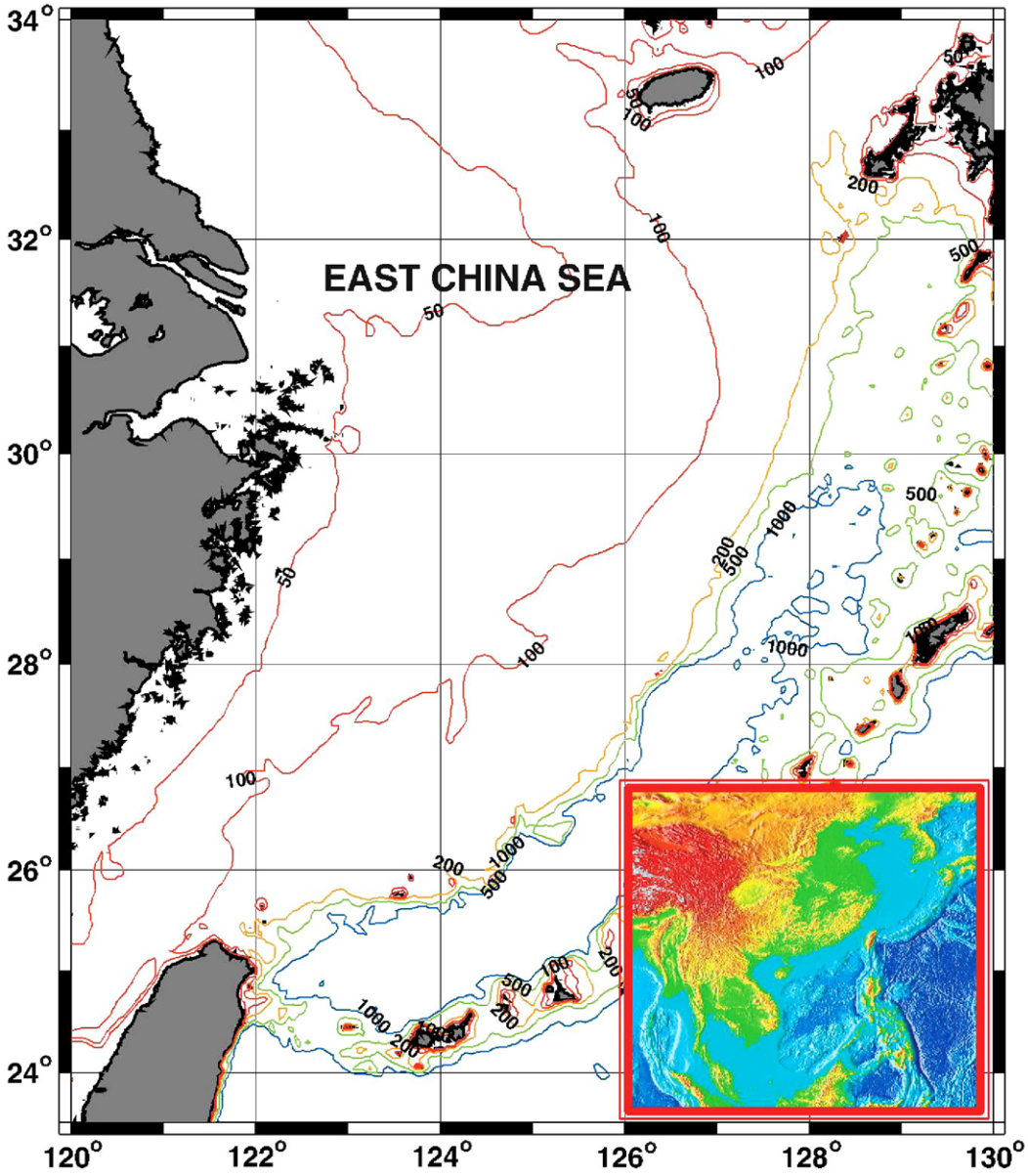

Fig. 2. The bathymetry map of the study area – The East China Sea between Taiwan and Korea.

persion was the PUS-SOG model of Cho and Lee (2006), except that we replaced the upper 5-km layer with layers that were, 0.5-, 1.5-, and 2.5-km thick for the thick sedimentary layer of East China Sea. In addition, the velocities of the model increased in a stepwise fashion from 2.9 to 3.4 km/s by 0.5 km/s. By including the velocity dispersion and starting with a regional crustal-upper-mantle model, we can produce a model that fits the dispersion. We inverted the observed dispersion using the program surf96 (Herrmann and Ammon, 2004).

We determined the structure of the profile between South Korea and Taiwan from the group velocity dispersion curve by inverting the data recorded at each station. To ensure that the path-averaged fundamental properties of the Rayleigh waves and Love waves relate to the crustal-upper mantle structure, we used all 19 recorded events through joint inversion.

We performed several inversion runs by separating the input data into different groups, to enable us to examine and compare the respective consistencies and convergence properties for the estimated dispersion curves. First, we inverted the group velocity data of the Rayleigh waves for the radial component. Second, we inverted the group velocity data of the Rayleigh waves for the vertical component. Third, we inverted the group velocity data of the Love waves for the transverse component. Finally, we performed a joint inversion of the group velocity data for all the available surface waves.

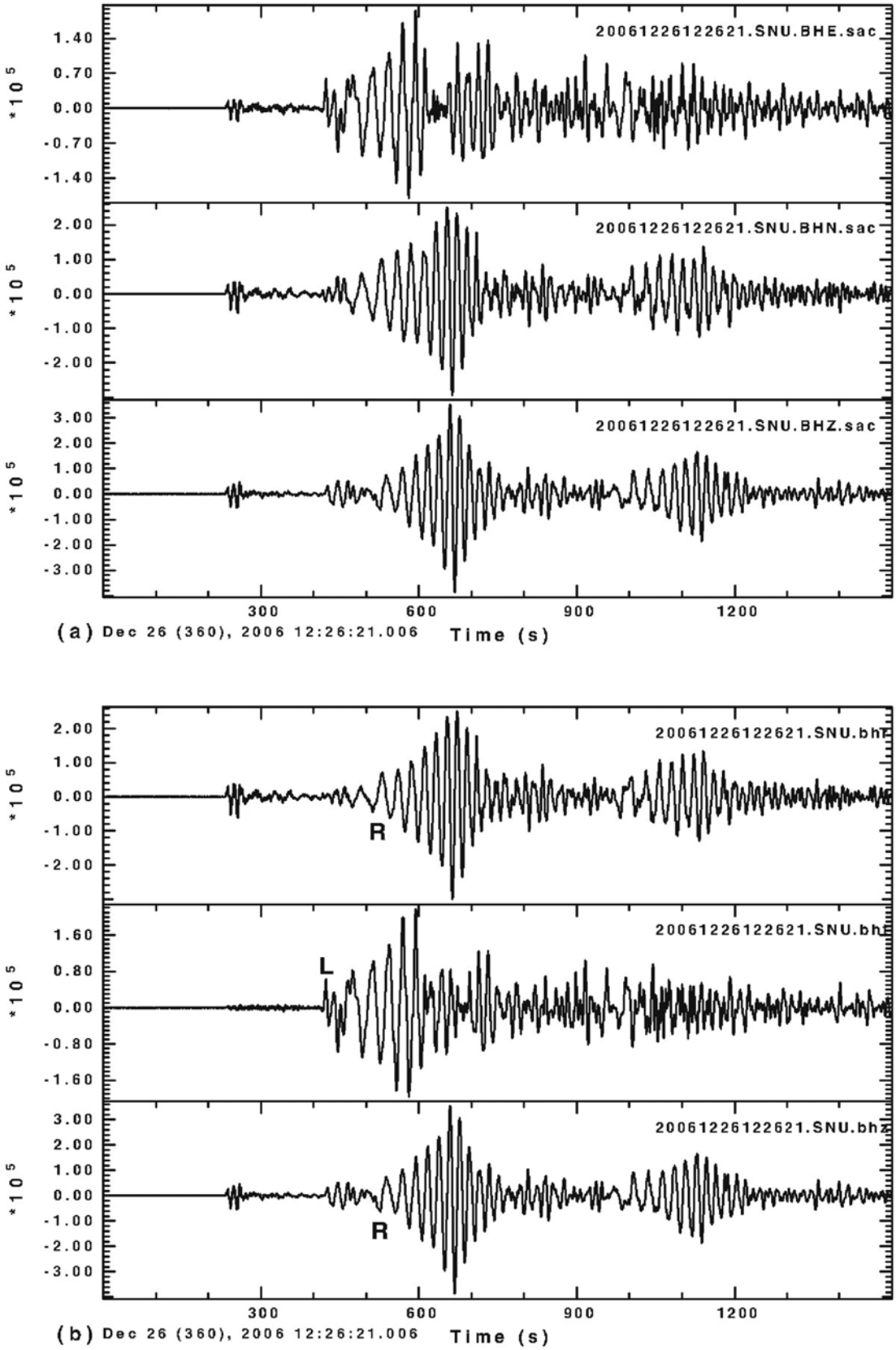

Fig. 3. A typical three component seismograms recorded from the PingTung earthquake doublets. (a) The recorded original seismograms from the SNU station for an event which occurred at 21.80°N and 120.55°E on 26 December 2006. (b) The processed seismograms after rotating along the great circle path from the original data in (a). L: Love waves; R: Rayleigh waves.

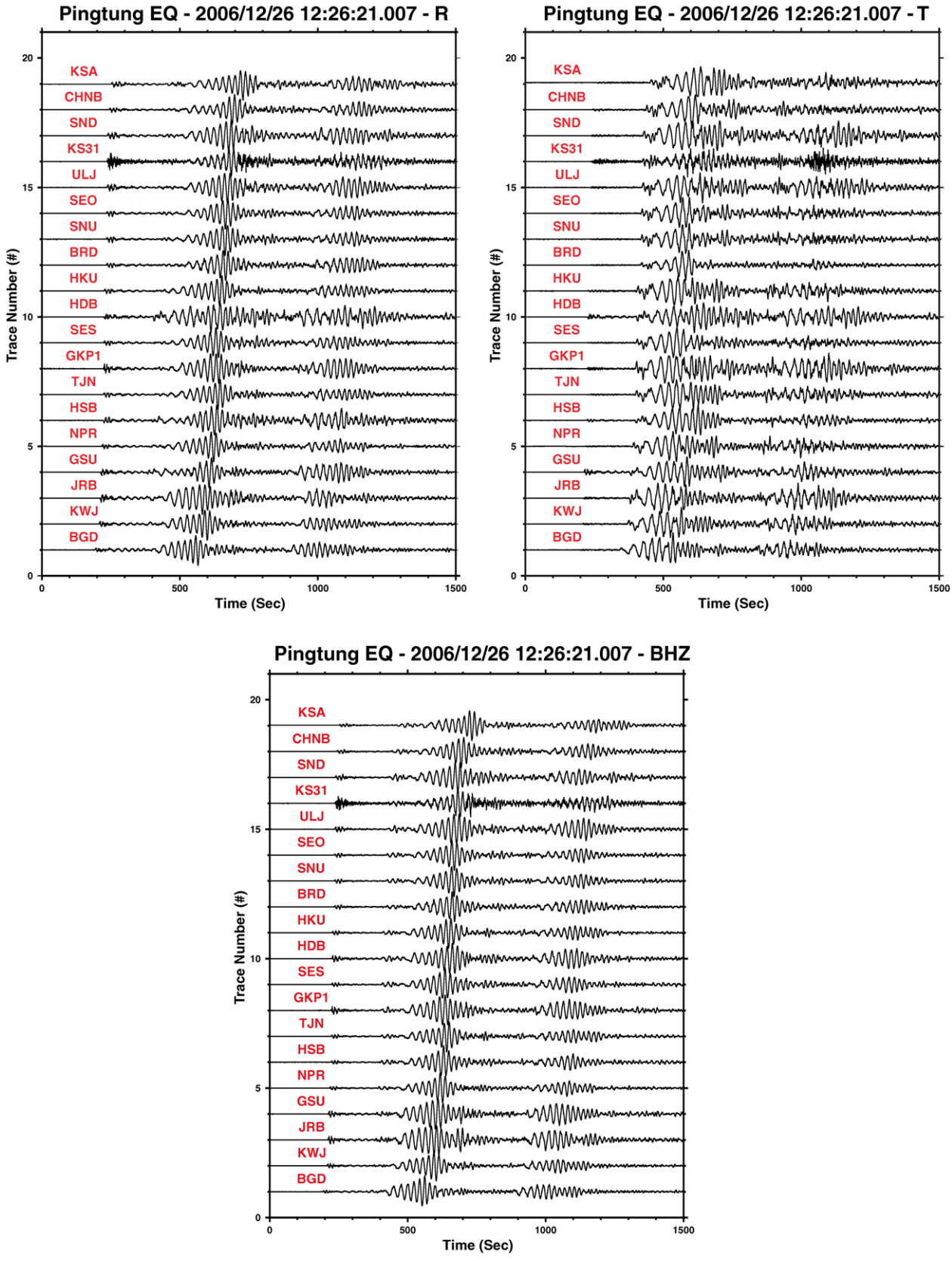

Fig. 4. Equally spaced three component seismograms recorded from the event occurring at 21.80°N and 120.55°E on 26 December 2006. The surface waves arriving approximately at 420 to 550 seconds at each station are the predominant phases. The seismograms are arranged according to their source-to-receiver distance to show the propagation effect across individual stations.

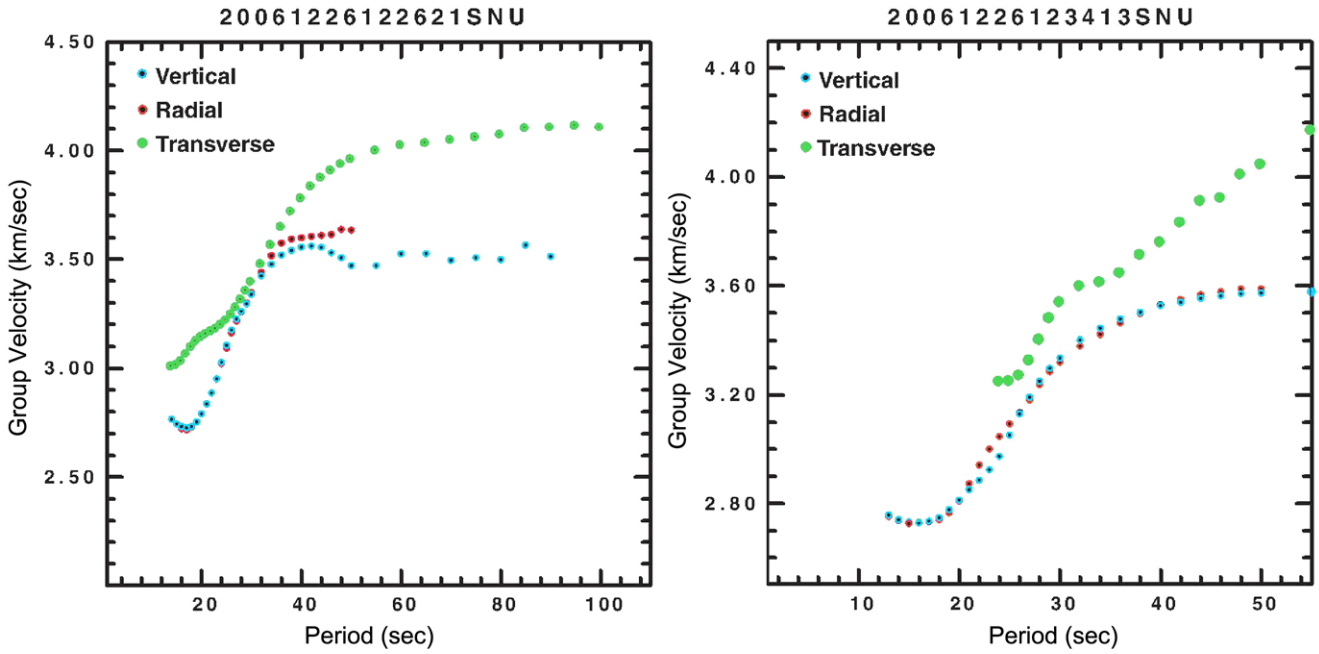

Fig. 5. Comparison of group velocity dispersion curves of Rayleigh waves from the vertical (blue dots) and radial component (red dots) and Love waves from the transverse component (green dots) at the SNU station for events that occurred at (a) 21.80°N and 120.55°E and (b) 21.97°N and 120.49°E on 26 December 2006.

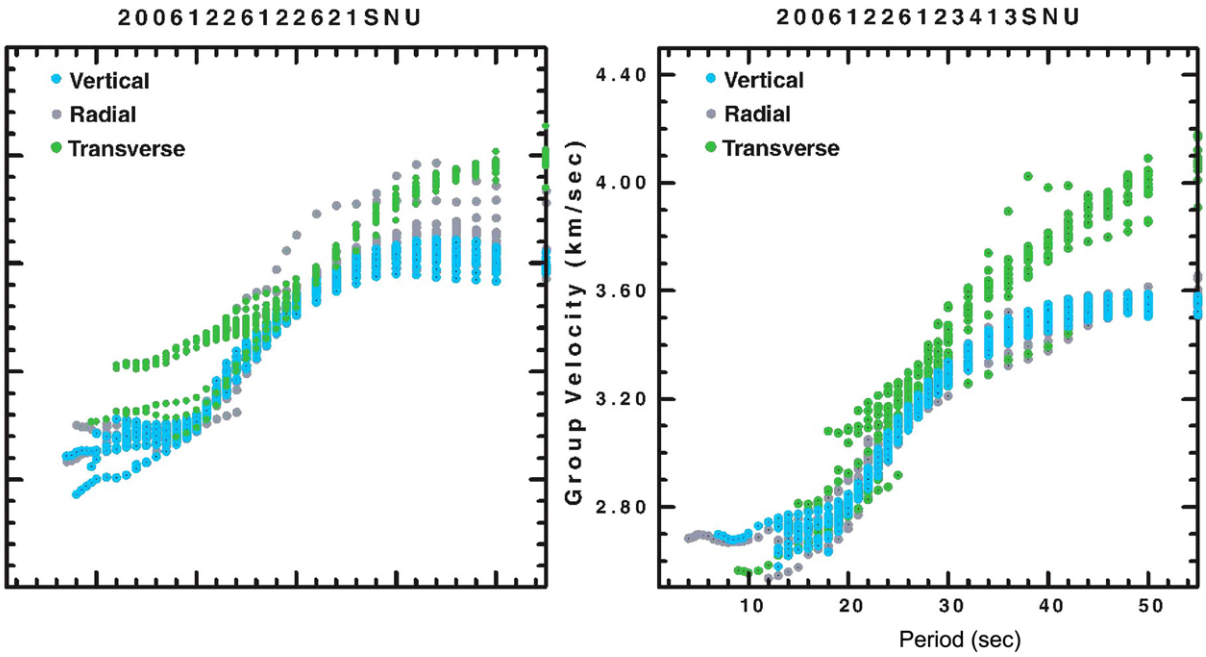

Fig. 6. Group velocity analysis for all the available data recorded from PingTung doublet earthquakes recorded at SNU broadband station. For the same event, distribution of group velocity variations for Rayleigh waves analysis from vertical (blue) and radial (gray) components are almost identical. Although the rupture behaviors are somewhat different, comparing the estimated group velocities from right (first event) to left (second event) is similar. For both events, a slightly higher Love wave dispersion property for the data from the transverse components (green) is shown.

Figure 7 shows the predicted theoretical dispersion curves, marked in red, as a result of a forward simulation of all the Rayleigh wave group velocities inverted from the radial (left) and vertical (right) components. The left panel of Figure 8 shows the calculated dispersion curve, which is estimated from inversion of the Love wave group velocity data. The right panel of Figure 8 shows the dispersion curves estimated from all available surface wave data. These curves

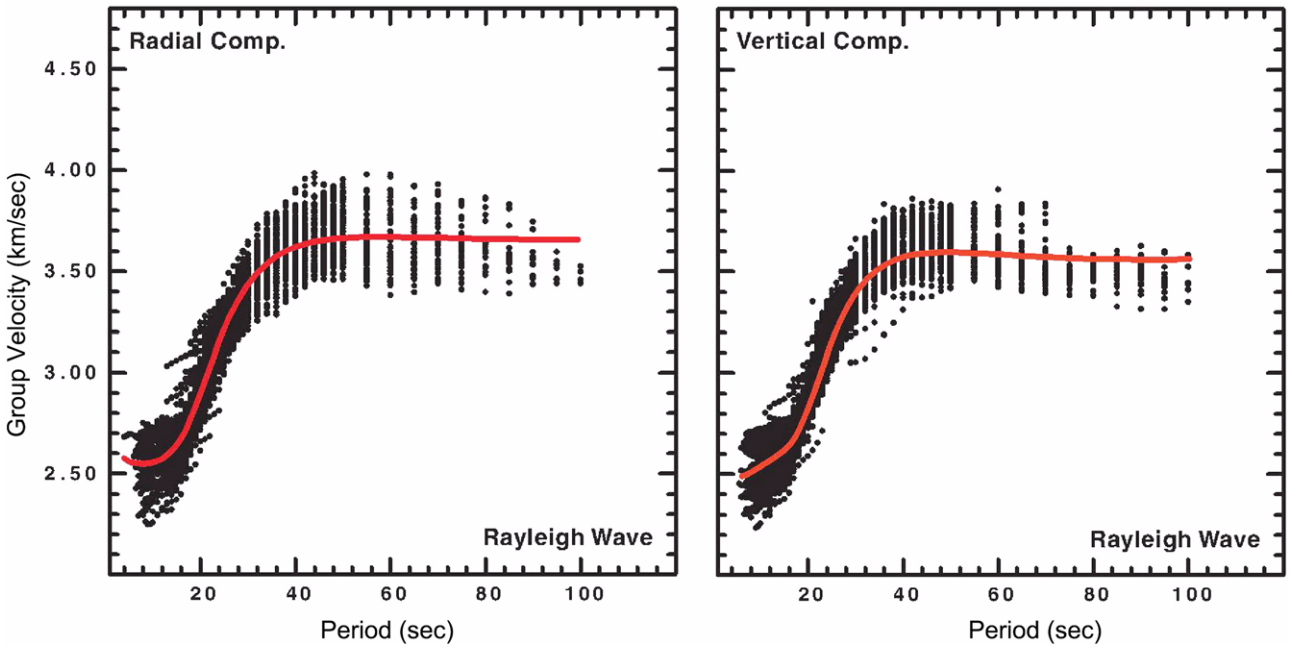

Fig. 7. The Rayleigh-wave dispersion curve (red line) predicted from the velocity structures resulting from the inversion. Rayleigh-wave group velocity data (black points) are estimated from the peak spectral amplitude of the processed radial component (left) and the originally recorded vertical (right) component through multiple filter analysis.

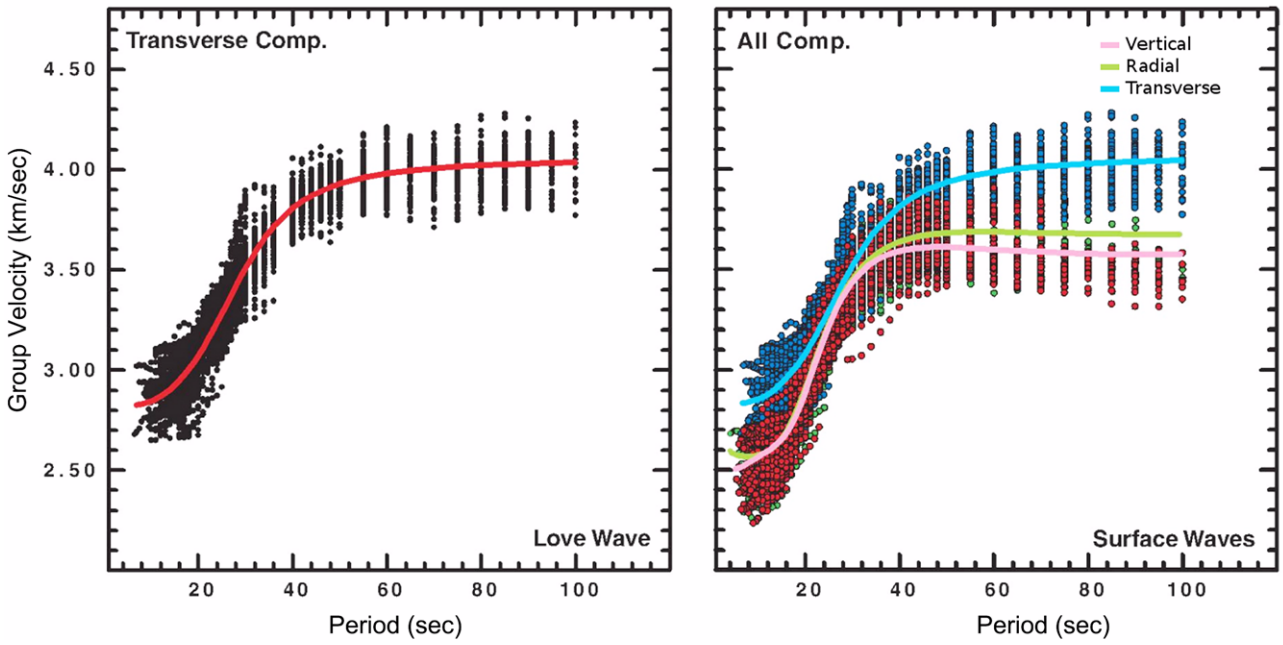

Fig. 8. Left panel shows the Love-wave dispersion curve (red line) predicted from the velocity structures resulting from the inversion with the use of all available Love-wave group velocity data (black dots) estimated from multiple filter analysis. Right panel shows the comparison of the simulated dispersion curves derived from the inversion of group velocity data from Rayleigh- and Love- waves. Distribution of group velocity variations for Rayleigh waves analysis from vertical (light red) and radial (light green) components is almost identical. A high velocity Love wave dispersion property for data inverted from the transverse component (light blue) is clearly shown.

exhibit a very clear distinction between Love waves and Rayleigh waves. Above a 60 s period, the Rayleigh wave group velocity dispersion curve from the radial component is slightly higher than that of the vertical component. Theoretically, the velocities of the Rayleigh waves from the radial and vertical components should be the same, although material anisotropy can account for the velocity differences. However, the group velocities for all the surface wave propagating paths are fairly consistent with each other, to within 0.5 km/s. The variation of group velocities shown in Fig-

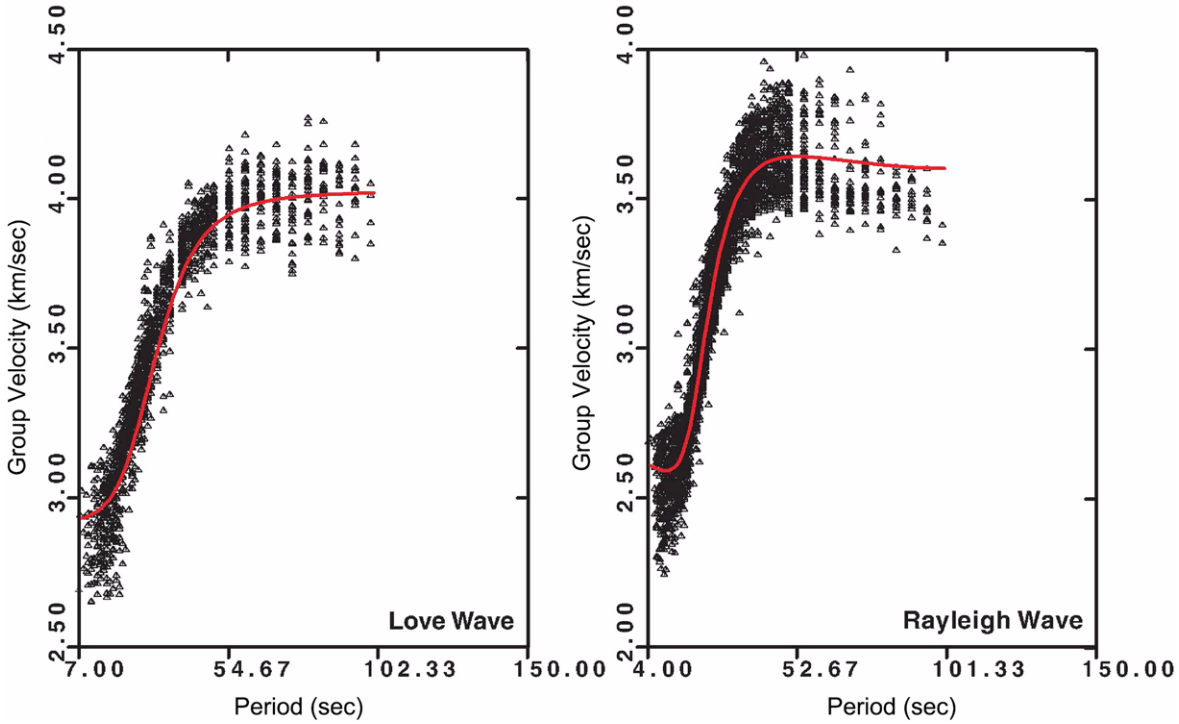

Fig. 9. The dispersion curves (red line) predicted from averaged velocity structures resulting from the joint inversion. All the available Love- (left) and Rayleigh- (right) wave group velocity data (black dots) were used to estimate the corresponding shear wave velocity profiles in the study area.

ures 7 and 8 can be attributed mainly to regional variations in surface-wave velocities. Therefore, the amount of variation in the observed group velocities is acceptable.

In Figure 8, although the Rayleigh wave dispersion curves below 60 s show similar group velocity properties, we require a more robust velocity-depth estimation for low-frequency surface waves traveling through the lower crust to the upper mantle. Therefore, we performed a joint inversion for the Rayleigh waves by combining data from both radial and vertical components. Figure 9 compares the predicted dispersion curves for both the Rayleigh wave (right) and Love wave (left) group velocities derived from all surface wave data through joint inversion. The predicted dispersion curves fit well from the group velocity data from the multiple filter analysis. In addition, the predicted Love wave dispersion curves show larger speeds than for Rayleigh waves in the study area. Because the forward problem is non-linear in terms of the model parameters, we performed an iterative sequence of linearized inversion, until the solution converged to a unified model. As iteration progresses, the model fit becomes better. To ensure the convergence falls into a global minimum, we show the velocity profiles from different datasets in Figure 10. The velocity structure derived from Rayleigh waves and Love waves are different, especially for high velocities jumping from the lower crust to uppermost mantle. The results mean that anisotropy can exist in this study area. Love waves are more sensitive to shear-wave velocity gradient changes than

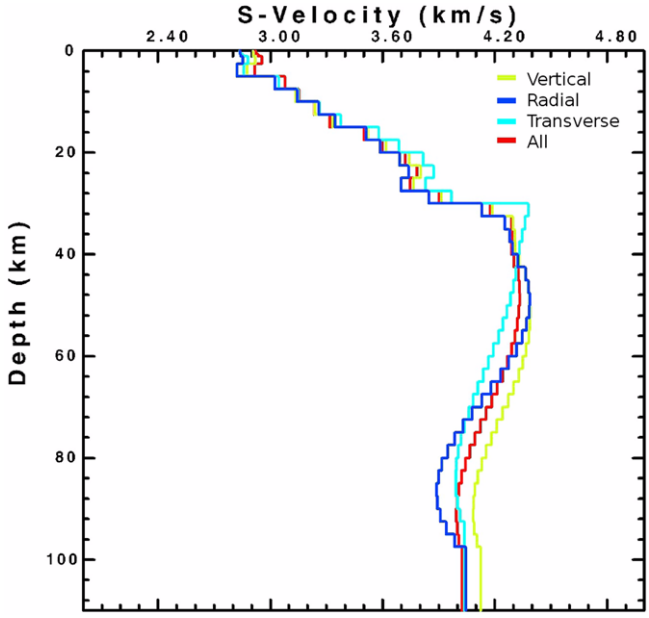

Fig. 10. Comparison of one dimensional shear wave velocity-depth functions estimated from radial (green) and vertical components (blue) and Love-wave group velocity (sky blue) datasets. A unified shear wave velocity profile (red) is also shown to represent the regional velocity variations through joint inversion estimated from all types of available data.

Rayleigh waves. A clear velocity discontinuity indicates that the Moho depth of about 30 km matched well with pre-

vious geophysical studies (Jiang et al., 2002; Lin et al., 2005; Han et al., 2007).

Now, we should discuss the average velocity structure between Korea and Taiwan using a statistical method such as the joint inversion of all data. Joint inversion using all the data of the Rayleigh waves and Love waves is very important to be able to reasonably estimate a resultant model, although the velocity structure of Rayleigh waves and Love waves is somewhat different. Therefore, our best shear velocity model (the red line from joint inversion) has features including: a surface layer, with a sediment thickness of 5 km and a shear velocity of 2.92 km/s, confirmed by previous local seismic and magnetic studies (Ludwig et al., 1973; Leyden et al., 1973; Hirata et al., 1991; Lin et al., 2005); a crust that appears to have a linearly increasing shear velocity gradient from 2.92 km/s at the top to 3.90 km/s at a depth of 30 km; a sharp shear-wave velocity discontinuity between the lower crust and upper mantle; and a smooth velocity variation from the upper mantle (4.33 km/s) down to 92.5 km (2.93 km/s), with a low-velocity zone (Table 2) at the lower portion of the lithosphere. We can infer that the crustal structure of the study area should mainly be continental crust.

Table 2. Average one dimensional shear wave velocity profile of the East China Sea obtained from the joint inversion

THICKNESS (KM)	VP (KM/S)	VS (KM/S)	RHO (GM/CC)
0.5	4.9704	2.9216	2.4940
0.5	4.9902	2.9331	2.4982
1.5	5.0337	2.9561	2.5069
2.5	4.9648	2.9166	2.4924
2.5	5.2424	3.0790	2.5487
2.5	5.3662	3.1519	2.5734
2.5	5.5088	3.2362	2.6018
2.5	5.6483	3.3185	2.6296
2.5	5.9604	3.5025	2.6919
2.5	6.1243	3.5984	2.7371
2.5	6.3321	3.7209	2.7996
2.5	6.4380	3.7830	2.8317
2.5	6.3777	3.7469	2.8139
2.5	6.6390	3.9001	2.8868
2.5	7.1079	4.1761	3.0155
2.5	7.2981	4.2881	3.0764
2.5	7.3089	4.2938	3.0799
2.5	7.3000	4.2895	3.0770
2.5	7.3207	4.3010	3.0836
2.5	7.3616	4.3259	3.0965
2.5	7.3704	4.3309	3.0992
2.5	7.3726	4.3321	3.0997
2.5	7.3664	4.3285	3.0976
2.5	7.3523	4.3202	3.0929
2.5	7.3298	4.3071	3.0856
2.5	7.2990	4.2890	3.0756
2.5	7.2618	4.2671	3.0637
2.5	7.2184	4.2417	3.0498
2.5	7.1707	4.2134	3.0346
2.5	7.1202	4.1839	3.0185
2.5	7.0682	4.1530	3.0020
2.5	7.0163	4.1229	2.9856
2.5	6.9670	4.0940	2.9719
2.5	6.9211	4.0668	2.9601
2.5	6.8803	4.0426	2.9497
2.5	6.8463	4.0230	2.9411
2.5	6.8204	4.0075	2.9345
2.5	6.8040	3.9979	2.9304
2.5	6.7975	3.9944	2.9289
2.5	6.8031	3.9975	2.9305
2.5	6.8203	4.0073	2.9351
0	6.8504	4.0256	2.9431

5. DISCUSSIONS AND CONCLUSIONS

We analyzed the path-averaged group velocity dispersion characteristics of Rayleigh waves and Love waves from 19 earthquakes with magnitude greater than 6.0, which occurred in Taiwan. The purpose of the study was to elucidate crust and upper-mantle structures of the region between Korea and Taiwan using the single-station method. The locations of the earthquakes used in this study are known and the focal parameters were determined by the USGS. The relative errors when determining the focal parameters are not expected to affect group velocities. We also note that the events used in this study are among the best-recorded earthquakes that have occurred in the Taiwan region. We would expect that epicentral location errors of these events are smaller than those of a typical event occurring in the Taiwan region. Therefore, for the range of the wave periods in our investigation, the effect on the source-group delays and mechanism is considered to be negligible. In general, the bathymetry map between Korean and Taiwan (Fig. 2) and the distribution of the picked surface wave group velocities (Figs. 9 and 10) suggest that, although some lateral variations occur across the region of interest, they are relatively minor. Judging from the waveforms shown in Figures 3 and 4, the effects from the existence of the water layer are relatively small, and can be ignored as a result of MFT analysis and surface-wave inversion. The analysis results of the dispersion curves, one dimensional velocity-depth functions inverted from individual group velocity picks, and all the available data also show persistent consistency.

The fundamental-mode group velocities of Rayleigh waves and Love waves across the East China Sea are determined to have a period of between 5 and 100 s. We used 19 events and data from 219 waveforms in our study of crust and upper mantle shear-wave velocity structures. Except for a relatively low near-surface S-wave velocity, we observed a near-linear velocity gradient in our study, with a zone of

thin, low velocity at the bottom of the crust. In the uppermost mantle, the model obtained from the inversion of the Love wave group velocity data has a higher velocity change than the inverted Rayleigh wave velocity profiles (Fig. 10). Beneath the high-velocity discontinuity, an apparent low-velocity zone exists, with a maximum velocity of 4.33 km/s. This gradually reduces to a minimum value of 3.99 km/s between 50 km and 92.5 km in depth. The Moho discontinuity is at a depth of 30 km, and we can clearly see an upper-mantle, low-velocity zone between 50 and 100 km from the results of this surface wave study. The average crustal structure of the study region is mainly a continental type. The thin lithosphere down to a depth of 50 to 60 km is above a pronounced low-velocity zone, which we interpret to be the low-viscosity asthenosphere. Future studies on the lower crust, mantle lithosphere, and upper asthenosphere down to 100 to 110 km will require further passive source data and measurements from South Korea.

ACKNOWLEDGMENTS: This study would not have been possible without the digital data sets provided by the Korea Institute of Geoscience and Mineral Resouces(KIGAM) and the Korea Meteorological Administration(KMA). This study was done by support of the Basic Research Project of KIGAM funded by the Ministry of Knowledge Economy of Korea. We thank editor and anonymous reviewers for their constructive comments.

REFERENCES

Cho, K.H. and Lee, K., 2006, Dispersion of Rayleigh waves in the Korean Peninsula. Journal of the Korean Geophysical Society, 9, 231–240.

Cho, K.H., Herrmann, R.B., Ammon, C.J., and Lee, K., 2007, Imaging the upper crust of the Korean peninsula by surface-wave tomography. Bulletin of Seismological Society of America, 97, 198–207.

Cho, K.H., Lee, S.-H., and Kang, I.-B., 2011, Crustal structure of the Korean Peninsula Using surface wave dispersion and numerical modeling. Pure and Applied Geophysics, doi: 10.1007/s00024-011-0262-x.

Dziewonski, A., Bloch, S., and Landisman, M., 1969, A technique for analysis of transient seismic signals. Bulletin of Seismological Society of America, 59, 427–444.

Fang, Y. and Liu, J., 2005, The crustal structure character of East China Sea. Marine Science Bulletin, 7, 2. (in Chinese with English abstract)

Han, B., Zhang, X., Pei, J., and Zhang, W., 2007, Characteristics of crust-mantle in East China sea and adjacent regions. Progress in Geophysics, 22, 376–382. (in Chinese with English abstract)

Herrmann, R.B., 1973, Some aspects of band-pass filtering of surface waves. Bulletin of Seismological Society of America, 63, 663–671.

Herrmann, R.B. and Ammon, C.J., 2004, Surface waves, receiver functions and crustal structure, in Computer Programs in Seismology. Version 3.30, Saint Louis University, http://www.eas.slu.edu/People/RBHerrmann/CPS330.html (last accessed December 12, 2006).

Hirata N., Kinoshita, H., Katao, H., Bada, H., Kaiho, Y., Koresawa, S., Ono, Y., and Hayashi, K., 1991, Report on DELP 1988 Cruises in the Okinawa Trough: Part 3. Crustal Structure of the Southern Okinawa Trough. Bulletin of the Earthquake Research Institute, University of Tokyo, 66, 37–70.

Jiang, W., Liu, S., Hao, T., and Song, H., 2002, Using Gravity Data to Compute Crustal Thickness of East China Sea and Okinawa Trough. Progress in Geophysics, 17, 35–41. (in Chinese with English abstract)

Leyden R., Ewing, M., and Murauchi, S., 1973, Sonobuoy refraction measurements in East China Sea. The American Association of Petroleum Geologists Bulletin, 57, 2396–2403.

Li, H., Liu, F., Sun, R., Zheng, Y., Peng, Y., and Huang, Z., 2001, Crust and upper mantle structure in east China and sea areas. Acta Seismologica Sinica, 14, 503–511.

Lin, J., Sibuet, J.-C., and Hsu, S., 2005, Distribution of the East China Sea continental shelf basins and depths of magnetic sources. Earth Planets Space, 57, 1063–1072.

Ludwing, W.J., Murauchi, S., Den, N., Buhl, P., Hotta, H., Ewing, M., Asanuma, T., Yoshii, T., and Sakajiri, N., 1973, Structural of East China Sea-West Philippine Sea margin off southern Kuyshu, Japan. Journal of Geophysical Research, 78, 2526–2536.

Nishida, K., Kawakatsu, H., and Obara, K., 2008, Three-dimensional crustal S wave velocity structure in Japan using microseismic data recorded by Hi-net tiltmeters. Journal of Geophysical Research, 113, B10302, doi:10.1029/2007JB005395.

Panza, G.F., Schwab, F., and Knopoff, L., 1973, Multimode surface waves for selected focal mechanisms – I. Dip-slip sources on a vertical fault plane. Geophysical Journal of the Royal Astronomical Society, 34, 265–278.

Panza, G.F., Schwab, F., and Knopoff, L., 1975a, Multimode surface waves for selected focal mechanisms – II. Dip-slip sources. Geophysical Journal of the Royal Astronomical Society, 42, 931–943.

Panza, G.F., Schwab, F., and Knopoff, L., 1975b, Multimode surface waves for selected focal mechanisms – III. Strike-slip sources. Geophysical Journal of the Royal Astronomical Society, 42, 945–955.

Yang, Y., et al., 2010, Rayleigh wave phase velocity maps of Tibet and the surrounding regions from ambient seismic noise tomography. Geochemistry, Geophysics, Geosystems, 11, Q08010, doi: 10.1029/2010GC003119.

Yoo, H.J., Herrmann, R.B., Cho, K.H., and Lee, K., 2007, Imaging the three-dimensional crust of the Korean Peninsula by joint inversion of surface wave dispersion and teleseismic receiver functions. Bulletin of Seismological Society of America, 97, 1002–1011.

Manuscript received October 6, 2009
Manuscript accepted February 23, 2011